Dyes and Pigments 95 (2012) 201–205

Contents lists available at SciVerse ScienceDirect

Dyes and Pigments

journal homepage: www.elsevier.com/locate/dyepig

Inkjet printable aqueous composite dye–polymer nanoparticles

Jonathan Henry Wilson [a], Roy Bradbury [b], Tom Annable [b], Stephen George Yeates [a,*]

[a] Organic Materials Innovation Centre, School of Chemistry, University of Manchester, Oxford Road, Manchester, M13 9PL, United Kingdom
[b] Fujifilm Imaging Colorants Ltd, Blackley, Manchester, M9 8ZS, UK

ARTICLE INFO

Article history:
Received 13 January 2012
Received in revised form
10 April 2012
Accepted 11 April 2012
Available online 20 April 2012

Keywords:
Inkjet
Nanoparticle
Encapsulation
Polymer
Dispersant
Anthraquinone

ABSTRACT

Here we report the synthesis of polymer stabilised anthraquinone dye-based aqueous nanoparticles using evaporative precipitation from dichloromethane into water and their use as novel aqueous inkjet colorants. Polymer stabilised dye nanoparticles in the 100 nm size range are demonstrated and the mechanism of formation of stable nanoparticles and the role of polymer stabiliser design is discussed. Formation of stable small particle size nanoparticles requires a fast dye crystal nucleation rate followed by a subsequent slow growth rate so as to avoid Ostwald ripening. Rapid nucleation can be achieved by metering small amounts of water-miscible organic solution of the dye to the non-solvent water under rapid mixing, referred to as quasi-emulsion solvent diffusion (QESD). These conditions result in high-supersaturation which causes spontaneous nucleation, followed by a rapid decrease in local supersaturation and hence slow crystal growth rate.

1. Introduction

Water insoluble crystalline disperse dyes have a broad colour gamut making them suitable for many high performance applications [1]. However their use in aqueous formulations requires either chemical modification, the use of energy intensive top-down dispersion methods using surfactants and/or polymeric dispersants, or appropriate polymer encapsulation [2–5]. Such processes usually involve mechanical force such as milling to achieve an appropriate particle size between 100 and 200 nm with no large particle size shoulder as required for robust inkjet printing.

In contrast bottom-up processing involves the formation of particles of the appropriate size from discrete molecules and as such a greater degree of control is possible [6,7]. Here we focus upon the use of evaporative precipitation which involves taking the dye of interest, dissolving it in a suitable solvent and on introduction to the aqueous continuous phase removal of the carrier solvent by evaporation leading to nanoparticle formation [8–12]. In synthesising nanoparticles based upon relatively hydrophobic crystalline disperse dyes two aspects need to be considered and controlled. Precipitation entails the creation of crystal nuclei, and their subsequent growth. Formation of stable small particle size nanoparticles requires a fast nucleation rate but slow growth rate so as to avoid Ostwald ripening [13]. Rapid nucleation can be achieved by metering small amounts of water-miscible organic solution of the dye to the non-solvent water under rapid mixing, referred to as quasi-emulsion solvent diffusion (QESD) [14]. These conditions result in high-supersaturation which causes spontaneous nucleation, followed by a rapid decrease in local supersaturation and hence slow crystal growth rate. In this paper we report the use of an evaporative precipitation technique involving the controlled metering of water-immiscible organic solvent containing dye and polymeric stabiliser into a temperature controlled aqueous solution with rapid solvent evaporation resulting in rapid and controlled dye-copolymer nanoparticle generation. Magenta H. 110300 (1-amino-4-hydroxy-2-[4-(1,1,3,3-tetramethyl-butyl)-phenoxy]-anthraquinone), Fig. 1) a hydrophobic crystalline dye (T_m = 171.5 °C) was chosen because of its low water solubility and good solubility in a range of organic water miscible and immiscible solvents including acetone and dichloromethane.

2. Experimental

2.1. Materials

1-Amino-2-bromo-4-hydroxyanthraquinone (C.I. Disperse Violet 17) (≥95%) was sourced from Advanced Technology and Industrial Company Ltd. and used without further purification. 2,2′-azobis(2-methylbutyronitrile) (Vazo 67) was kindly donated by Fujifilm Imaging Colorants Ltd. and was used as supplied.

* Corresponding author. Tel.: +44 (0) 161 2751421; fax: +44 (0) 161 2754273.
E-mail address: Stephen.Yeates@manchester.ac.uk (S.G. Yeates).

0143-7208/$ – see front matter © 2012 Elsevier Ltd. All rights reserved.
doi:10.1016/j.dyepig.2012.04.005

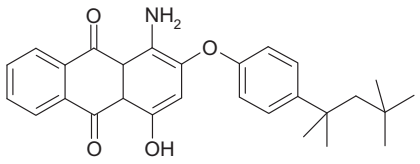

Fig. 1. Magenta H. 110300 (1-amino-4-hydroxy-2-[4-(1,1,3,3-tetramethyl-butyl)-phenoxy]-anthraquinone).

Methylmethacrylate (MMA), methacrylic acid (MAA) and 2-ethylhexylmethacrylate (EHMA) and all other reagents were obtained from Sigma Aldrich UK and used as received.

2.2. Characterisation

Molecular weights were measured using a Viscotek size exclusion chromatograph instrument equipped with 3 PLgel 10 μm Mixed-B columns and a differential refractive index detector. The eluent was tetrahydrofuran (THF) at a flow rate of 1 ml min^{-1} and the system was calibrated using polystyrene standards. ^1H NMR spectra were recorded using a 500 MHz Bruker. FT-IR spectra were obtained using a BioRad 'Excalibur' ATR-FT-IR spectrometer. Photocorrelation spectroscopy (PCS) particle sizing was performed in water using a Zetasizer-Nano from Malvern Instruments. Particle size (ps) and dispersity (PDi) were analysed assuming a monomodal distribution. For PDi $>$ 0.2 particle diameter is quoted and for PDi $<$ 0.2 'z-average' is quoted. Differential Scanning Calorimetry (DSC) was performed using a Perkin–Elmer Diamond DSC. Cryo Environmental Scanning Electron Microscopy (CESEM) was performed using a Philips ESEM XL30, 5–10 keV. Samples were prepared by adding a small amount to a sample tube, cooling rapidly in liquid nitrogen and cutting the tube in half. The cryogenically frozen surface is then coated with gold and viewed in a sample chamber held at around −130 °C. Powder diffraction was performed using a Philips Xpert station with a Cu K_α source at 1.5405980 nm. Ink-jet printing was carried out using a Dimatix DMP-2800 inkjet printer (Fujifilm Dimatix, Inc., Santa Clara, USA) fitted with a waveform editor and a drop-watch camera system which allows manipulation of the electronic pulses to the piezo jetting device for optimization of the drop characteristics as it is ejected from the nozzle. The nozzle plate consists of a single row of 16 nozzles of 23 μm diameter spaced 254 μm with typical drop size of 10 pl and drop diameter 27 μm. CIE colour space was measured on a Minolta CR-300 chroma meter colorimeter calibrated with a white card which had colour space of 0.3136 (x), 0.3194 (y) and 92.5 (Y).

2.3. Synthesis of Magenta H 110300: (1-amino-4-hydroxy-2-[4-(1,1,3,3-tetramethyl-butyl)-phenoxy]-anthraquinone)

1-Amino-2-bromo-4-hydroxyanthracene-9,10-dione (C.I. Disperse Violet 17) (0.05 mol, 15.91 g), 4-tert-octyl phenol (0.5 mol, 103.17 g, 10 fold excess) and potassium carbonate (0.055 mol, 7.60 g) were combined and stirred at 150 °C for 15 h at which point all the C.I. Disperse Violet 17 had been consumed as analysed by TLC (hexane:diethyl ether; 3:1). The reaction mixture was cooled to 90 °C, and 180 ml of methanol slowly added causing the deep red product to precipitate. The reaction mixture was cooled to room temperature and the product filtered off. The product was washed four times with methanol and four times with deionised water, and dried under vacuum overnight yielding 1-amino-4-hydroxy-2-[4-(1,1,3,3-tetramethyl-butyl)-phenoxy]-anthraquinone as a deep red solid in 84% yield (18.70 g). Elemental analysis: Calculated (%) C 75.8, H 6.55, N 3.2; found C 74.72, H 6.55, N 3.07. ^1H NMR ($CDCl_3$) δ (ppm): 0.78 (br.s., 9H), 1.43 (br.s., 6H), 1.80 (br.s., 3H), 6.42 (br.s., 1H), 7.09 (br.s., 2H), 7.49 (br.s., 2H), 7.79 (s., 2H), 8.38 (br.s., 2H), 14.16 (br.s)., 1H. Melting point: 170.3 °C.

Calculated solubility parameters; δ_p = 4.5 $MPa^{1/2}$, δ_d = 23.8 $MPa^{1/2}$, δ_h = 10.6 $MPa^{1/2}$ [15], log P = 7.5 +/− 0.8 at 25 °C and log D = 7.5, 7.4, 7.1, 6.3 and 5.4 at 25 °C and pH 5, 6, 7, 8, and 9 respectively [16].

2.4. Polymer synthesis

Statistical methacrylate copolymers were prepared using starve fed free-radical solution polymerisation. Each copolymer contained MAA, which when neutralised with 0.98 equivalents triethylamine provided the charge-based stabilisation required to maintain a finely divided dispersion. The main chain hydrophobic component, MMA and EHMA, was chosen so as to have differing affinities for the hydrophobic substituted anthraquinone dye based upon solubility parameter considerations. Compositions were chosen using established polymer dispersant and inkjet design principles [17–23], such that [MAA] = 17.5 wt-%, M_n = 16–24 kDa, PDi typically between 2–3, and overall hydrophobicity defined using a calculated Hansch Parameter, Log P in the range of 0.54–3.75 [21]. Calculated glass transition temperatures (Tg) were in the range 122 °C (**P1**) and 14 °C (**P9**).

The following synthetic methodology was used for all copolymers in the study. Polymer **P5**: Propan-2-ol (28.13 g) was added to the reaction flask, heated to reflux for 30 min and separate solutions of propan-2-ol (18.75 g) and Vazo 67 (0.0078 mol, 1.5 g) and propan-2-ol (28.13 g), MMA (0.358 mol, 38.85 g), EHMA (0.132 mol, 26.25 g) and MAA (0.150 mol, 12.90 g) fed into the reaction flask over 2 h while the temperature in the flask was held at 83 °C. Once addition was complete, the reaction was maintained at 83 °C for a further 4 h before being cooled to room temperature and a further amount of propan-2-ol (75 g) added and stirred until homogeneous. The polymer was isolated by precipitation into ice chilled water and collection by filtration. The polymer was dried under vacuum, yielding a fine white powder at 75.5% yield (65.3 g).

2.5. Dye–polymer dispersion

The following describes the final optimized process as assessed by small nanoparticle size and stability to sedimentation using dichloromethane (DCM) as volatile organic solvent. To 80 ml of distilled water, held at 80 °C stirred at a rate of 250 rpm using an overhead stirrer with a centrifugal impeller blade, 20 ml of an 80:5:15 DCM:dye:polymer (w/w) (polymer pre-neutralised with 0.98 equivalent triethylamine) was passed through a heated hot bath at 80 °C and injected at a flow rate of 2 ml min^{-1} using uncoated stainless steel GC tubing having an internal diameter of 0.01 inches with an end tip diameter of 1/16 inch placed 1 cm under the surface of the water. DCM was collected using a Dean and Stark condenser and upon complete removal the total solids content was adjusted to 5 wt-% by the addition of the appropriate amount of distilled water.

3. Results and discussion

3.1. Solvent evaporation method for the formation of dye–polymer nanoparticles

Particle size and resultant stability to sedimentation of dye–polymer nanoparticles prepared using evaporative precipitation were found to be highly process dependent. Nanoparticle dispersion quality was evaluated visually and by PCS particle size

Table 1
Key copolymer compositions and characterization, and particle size information for 1:3 w/w dye–polymer nanoparticles in water prepared by method described in Section 2.4.

	MMA (wt-%)	EHMA (wt-%)	MAA (wt-%)	M_n[a] (kDa)	Log P[b]	Calc Tg (°C)	Particle Size (nm)[c]	PDi[c]
P1	82.5	0	17.5	16.8	1.09	122	270	0.34
P2	77.5	5	17.5	26.9	1.23	113	215	0.11
P3	67.5	15	17.5	20.6	1.5	97	170	0.12
P4	57.5	25	17.5	22.9	1.78	82	130	0.14
P5	47.5	35	17.5	16.4	2.06	68	115	0.18
P6	27.5	55	17.5	23.3	2.61	43	240	0.35
P7	17.5	65	17.5	22.6	2.89	32	140	0.23
P8	7.5	75	17.5	19.7	3.16	21	100	0.24
P9	0	82.5	17.5	23.9	3.38	14	190	0.37

[a] Polystyrene equivalent molecular weight.
[b] Calculated overall Hansch Parameter [17].
[c] Particle size as measured by PCS (+/− 10 nm) from an average of at least different particle synthesis.

analysis. Initial process analysis was performed using 20 ml solvent:dye:**P5** 80:5:15 w/w feed solution added to 80 ml of aqueous phase with agitation. In all cases when the aqueous phase was held at 25 °C this lead to formation of unstable large aggregates. Similarly injecting the dye–polymer solution at a temperature just below the boiling point of the solvent gives the most stable particles. The best volatile organic solvent are those that are a good solvent for both dye and stabilising polymer, have very low water solubility and have a boiling point such that on introduction to the heated aqueous phase is rapidly and efficiently removed. DCM was found to best fit these criteria, with solvents of increasing water miscibility giving nanoparticles having particle size (ps) > 500 nm which were unstable to sedimentation overnight at 25 °C. Optimisation studies showed that pre-dissolution of the pre-neutralised polymeric stabiliser in DCM with dye yielded the most stable nano-suspensions having the smallest particle size. This is believed to be due to the close admixture of polymer and dye at the point of dye precipitation leading to rapid stabilisation so reducing the tendency to Ostwald ripening. Similarly it was found that injecting the dye–polymer solution at a temperature just below the boiling point of DCM (38–40 °C) into water held at 80 °C resulted in rapid solvent evaporation and stable nanoparticle dispersion particle size = 113 nm, PDi = 0.18.

The feed rate of DCM solution into water over the range 0.3–6 ml min^{-1} was found not to have an effect on dispersion particle size or stability. In order to minimise foam formation during dispersion dye solution feed rates were kept below 2 ml min^{-1}. Agitation of the aqueous phase using a two-blade centrifugal type impeller at a rate of 250–500 rpm was found to give reproducible results with lower rates yielding larger particle size and higher rates resulting in foam formation. Whilst the optimum ratio of DCM:dye:polymer was found to be 80:0.5:1.5 w/w giving a particle size = 103 nm, PDi = 0.17 the improvement in nanoparticle dispersion quality compared with 80:5:15 w/w was not significant to offset the significant decrease in dye loading. Similarly, a dye–polymer ratio of 1:3 w/w was found to give the best nanoparticle dispersion quality.

Mono-modal particle size measured by PCS as a function of copolymer Log P for dye–polymer nanoparticles at 1:3 w/w are given in Table 1 and plotted in Fig. 2a, with CESEM confirming that the particles are essentially spherical over the whole range, Fig. 2b. This shows a strong dependence of particle size on copolymer composition with two identified particle size minima. The first at a copolymer composition of MMA/EHMA/MAA = 47.5/35/17.5 (**P5**) equating to an overall copolymer hydrophobicity of Log P = 2.0, and the second local minima at MMA/EHMA/MAA = 7.5/75/17.5 (**P8**) equating to an overall copolymer hydrophobicity of Log P = 3.15. Dispersion stability is a subtle balance between the ability of the copolymer dispersant to adsorb and interact with the disperse dye during the particle formation process whilst at the same time having appropriate hydrophilicity to extend into the aqueous phase and provide sufficient ionic/steric stabilisation. For all copolymers the zeta potential was measured between −80 and −70 mV and did not change over 30 days at 25 °C. From consideration of the monomer reactivity ratios the copolymers are essentially statistical in nature. The first stable particle size minimum (**P5**) is believed to correspond to the copolymer composition having the optimum hydrophilic-hydrophobic to give a high degree of ionic/steric stabilisation [17–21]. The second stable particle size minimum (**P8**) is believed to correspond to the case where the more hydrophobic segment interacts most strongly with the disperse dye during the particle formation process whilst retaining sufficient ionic/steric stabilisation.

3.2. Nanoparticle morphology

X-ray powder diffraction analysis of 1:3 w/w dye–polymer nanoparticles showed that for all copolymers the nanoparticles contain both crystalline and amorphous dye, Fig. 3a. DSC has been widely used to study drug–polymer interactions [24]. Through analysis of the melting point of pure dye in dye–polymer solution cast blends and nanoparticles (**P5** and **P8**) we observe that the

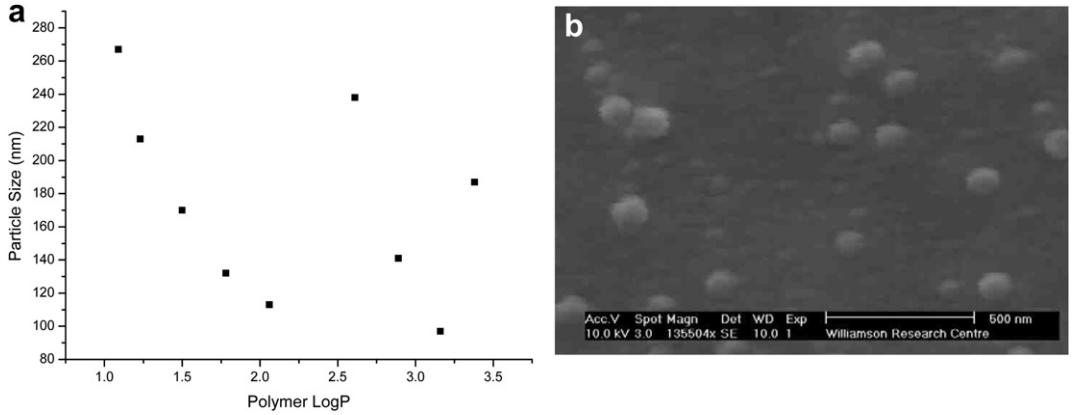

Fig. 2. (a) Nanoparticle dye–polymer = 1:3 w/w particle size as measured by PCS (+/− 10 nm) as a function of calculated polymer Log P [25]. (b) CESEM of nanoparticle 1:3 w/w dye-**P5**.

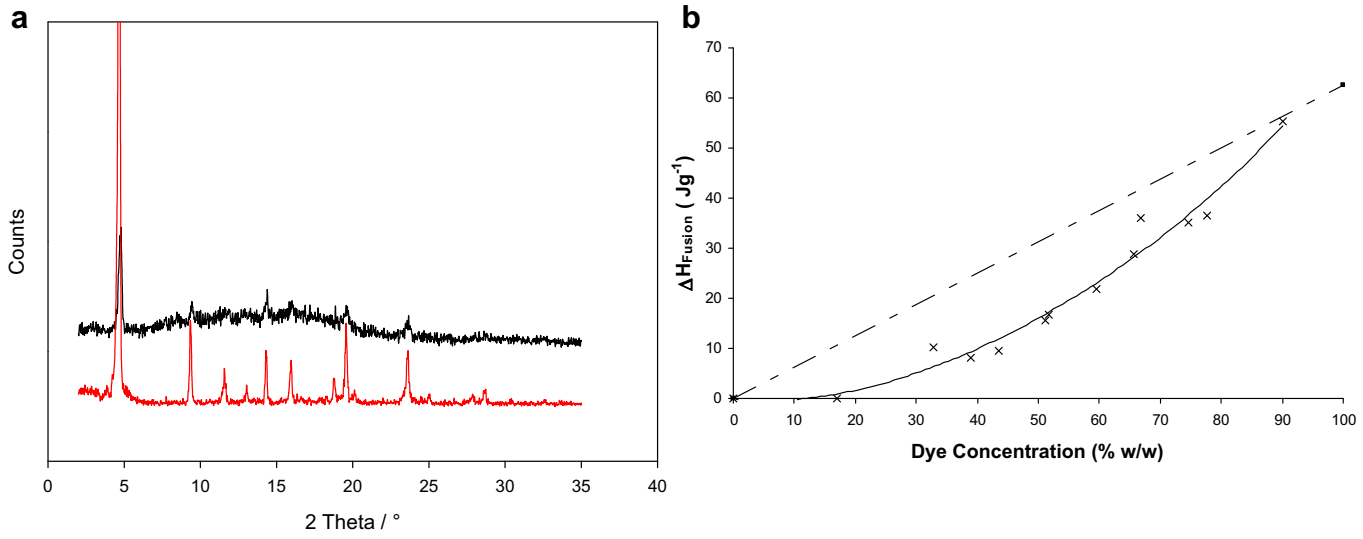

Fig. 3. (a) XRD powder diffraction of 1:3 w/w dye-**P5** nanoparticle (top) and pure Magenta H. 110300 (bottom). (b) Measured enthalpy of fusion ($\Delta H_{fusion}/Jg^{-1}$) from DSC run at 20 °C/min for dye-**P5** solution cast blends (–) and calculated enthalpy of fusion (-.-) based upon value obtained for pure dye.

measured enthalpy of fusion at the melting point (ΔH_{fusion} (J g^{-1})) is less than that calculated assuming full dye crystallisation for polymer contents > 10 wt-%, Fig. 3b. For dye-**P5** nanoparticle at 1:3 w/w ratio $\Delta H_{fusion} = 4$ J g^{-1} indicating that approximately 25% of the available dye is crystalline, and for dye-**P8** nanoparticle at 1:3 w/w ratio $\Delta H_{fusion} < 2$ J g^{-1} indicating that less than 10% of dye is crystalline. Detailed inspection of the shape and position of the melting endotherm of the dye in dye–polymer nanoparticles as a function of dye loading show subtle differences for polymers **P5** and **P8**, Fig. 4(a and b).

Both polymers show that at high dye concentrations the endotherms are close to that of the pure dye consistent with dye–dye interactions dominating [25,26]. At low dye concentrations dye–polymer interactions become increasingly important. Insight into the miscibility or otherwise of the respective dye–polymer blends is potentially forthcoming from consideration of the respective solubility parameters which take into account the relative strengths of the dispersion (δ_d), polar (δ_p) and hydrogen bonding (δ_h) forces [27,28]. Due to difficulties in dealing with the ionized methacrylic acid segment different calculation methods give different rank order in terms of dye–polymer miscibility. Hoftzer-van Krevelen [27] and Hansen [28] indicate slightly more favourable interaction between dye and **P5**, whilst Hansen [28] slightly favours dye and **P8**. It is to be noted however that nanoparticle formation is performed at 80 °C just above the Tg of **P5**, 68 °C, and well above that of **P8**, 21 °C. This may well be an important consideration in the later stages of nanoparticle formation when the majority of DCM has been removed and hence influence the rate of dye diffusion and crystal growth.

3.3. Inkjet printing

The jet ability of a 1:3 dye-**P5** nanoparticle ink formulated having a viscosity of 2.5 cps at 25 °C and surface tension of 33.0 mN m^{-1} at 25 °C [29] comprising 1:1 v/v water: ethanol equating to a total solids content of 2.5 wt-% and a dye loading of 0.625 wt-%. was evaluated using a Dimatix DMP 10 pl nozzle. With a 50 μm drop spacing, squares of 0.5 × 0.5 × 0.5 cm were reproducibly printed with either 1, 2 and 3 passes onto Melinex 300, and with no nozzle blockage. To test the wet-fastness of the

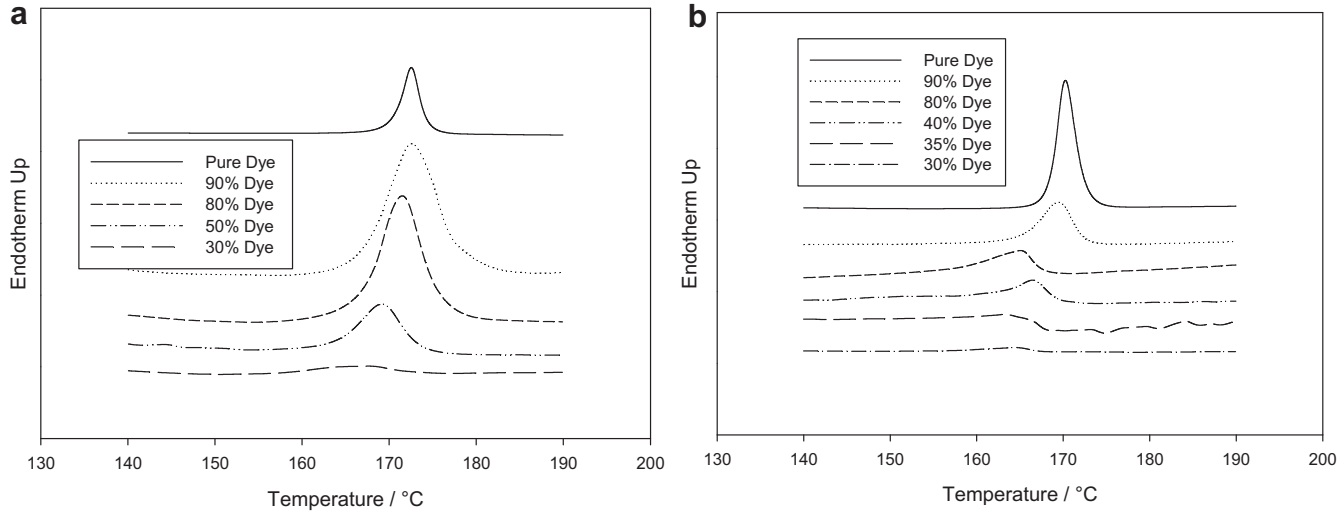

Fig. 4. DSC thermogram of (a) dye-**P5** and (b) dye-**P8** nanoparticles at varying dye–polymer compositions run at 20 °C/min.

Table 2
CIE xyY colour space of 1:3 dye-**P5** nanoparticle ink printed 1, 2 and 3 passes onto Melinex 300.

Number of prints	x	y	Y
1	0.317	0.324	76.09
2	0.323	0.321	71.60
3	0.327	0.318	68.98

printed image, after being allowed to dry for 1 h, a wet cloth was rubbed over the printed image and in all cases no smearing or bleeding of the colour was observed. The CIE xyY colour co-ordinates were determined and are given in Table 2 and compared with those for pure Magenta H 110300; 0.565 (x), 0.287 (y) and 4.5 (Y). It can be seen that the nanoparticle dye shows colour in the blue-red region the difference between the pure Magenta H 110330 being as a consequence of different physical interactions with the substrate [30].

4. Conclusions

Reproducible copolymer stabilised aqueous hydrophobic dye nanoparticles in the 100 nm size range have been prepared by a solvent evaporation method are demonstrated. The nanoparticle morphology is consistent with domains of crystalline dye in an amorphous dye–polymer matrix, with the percentage of dye crystallisation within the nanoparticle decreasing at high copolymer weight fractions. Copolymer composition is critical with respect to nanoparticle stabilisation and the nature and extent dye-copolymer interaction. A number of parameters influencing the final particle morphology are identified and these need to be considered holistically when designing a robust process whilst retaining control over final particle morphology and properties. Resultant nanoparticles were capable of being robustly inkjet printed.

Acknowledgements

JHW would like to thank EPSRC and Fujifilm Imaging Colorants Ltd for funding.

References

[1] Fryberg M. Review of Progress in Coloration 2005;35:1–30.
[2] Chang SYP, Chao YC. Journal of Imaging Science and Technology 2007;51:413–8.
[3] Lee JJ, Lee WJ, Choi JH, Kim JP. Dyes and Pigments 2005;65:75–81.
[4] Fu S, Zhang G, Du C, Tian A. Journal of Applied Polymer Chemistry 2011;121:1616–21.
[5] Fu S, Xu C, Du C, Tian A, Zhang M. Colloids and Surfaces A: Physiochemical and Engineering Aspects 2011;384:68–74.
[6] Rabinow BE. Nature Reviews Drug Discovery 2004;3:785–96.
[7] Patravale VB. Journal of Pharmacy and Pharamacology 2004;56:827–40.
[8] Bodmeier R, Chen HJ. Controlled Release 1990;12(3):223–33.
[9] Chen X, Young TJ, Sarkari M, Williams RO, Johnston KP. International Journal of Pharmaceutics 2002;242(1–2):3–14.
[10] Dailey LA, Schmehl T, Gessler T, Wittmar M, Grimminger F, Seeger W, et al. Controlled Release 2003;86(1):131–44.
[11] Oh KT, Bronich TK, Kabanov AVJ. Controlled Release 2004;94(2–3):411–22.
[12] Hernandez-Trejo N, Kayser O, Steckel H, Mueller RHJ. Drug Targeting 2005;13(8–9):499–507.
[13] Castelli F, Messina C, Sarpietro MG, Pignatello R, Puglisi G. Thermochimica Acta 2003;400(1–2):227–34.
[14] Sarkari M. International Journal of Pharmaceutics 2003;243(1–2):17–31.
[15] Hansch C. Accounts of Chemical Research 1969;2(8):232–9.
[16] Calculated using Advanced Chemistry Development (ACD/Labs) Software V11.02 (© 1994-2011 ACD/Labs).
[17] Tadros ThF. Advances in Colloid and Interface Science 1980;12(2–3):141–261.
[18] Spinelli HJ. Advanced Materials 1998;10(15):1215–8.
[19] US 5821283, Rohm and Haas.
[20] Merrington J, Hodge P, Yeates SG. Macromolecular Rapid Communications 2006;27(11):835–40.
[21] Merrington J, Yeates SG, Hodge P, Christian P. Journal of Materials Chemistry 2008;18:182–9.
[22] Xu D, Sanchez-Romaguera V, Barbosa S, Travis W, de Wit J, Swan P, et al. Journal of Materials Chemistry 2007;17:4902–7.
[23] A.-Alamry K, Nixon K, Hindley R, Odel JA, Yeates SG. Macromolecular Rapid Communications 2011;32(3):316–20.
[24] Gramaglia D, Conway BR, Kett VL, Malcolm RK, Batchelor HK. International Journal of Pharmaceutics 2005;301(1–2):1–5.
[25] Slark AT, Hadgett PM. Polymer 1998;39(10):2055–60.
[26] Slark AT, Hadgett PM. Polymer 1999;40(14):4001–11.
[27] Krevelen DWV. Properties of polymers. 3rd ed. Elsevier; 1997. p. 212.
[28] Barton AFM. Handbook of solubility parameters and other cohesion parameters. CRC Press; 1985.
[29] Sanchez-Romaguera V, Madec M-B, Yeates SG. Reactive & Functional Polymers 2008;68(6):1052–8.
[30] Grabchev I, Philipova T. Dyes and Pigments 1998;39(2):89–95.